Development of a Semiautomated Zero Length Column Technique for Carbon Capture Applications

Development of a Semi-Automated Zero Length Column Technique for Carbon Capture Applications: Rapid Capacity Ranking of Novel Adsorbents.

Xiayi Hu[1], Stefano Brandani[1]†, Annabelle I. Benin[2] and Richard R. Willis[2]*

1. Institute for Materials and Processes, School of Engineering, the University of Edinburgh, UK

2. New Materials Research, UOP LLC, a Honeywell Company, Des Plaines, IL, USA

† Corresponding author. Email address: s.brandani@ed.ac.uk

* Current address:
College of Chemical Engineering, Xiangtan University, Hunan Province, 411105, P. R. China

ABSTRACT

A novel zero length column (ZLC) apparatus has been developed to provide rapid screening of CO_2 capacities of adsorbent materials. The key features of the new apparatus are the use of 5-15 mg of sample, a purposely designed gas-dosing system and low flowrates that extend the use of the ZLC to test adsorbents for post-combustion for carbon capture applications.

The new ZLC system was first applied to provide rapid screening capacity ranking of more than 15 MOF materials and three representative zeolites. At the point of interest for flue gas application (38°C, 0.1 bar CO_2 partial pressure), Mg/DOBDC was found to outperform significantly all other MOFs and the benchmark zeolites.

Key words: Zero length column (ZLC), adsorption, MOFs, CO_2 capture, ranking

INTRODUCTION

CO_2 capture and storage from flue gases will play a significant role in mitigating the effect global warming on climate change. Coal-fired power plants produce more than 40 percent of CO_2 emissions and as such are attractive targets for capture technologies.[1] Normally power plants produce flue gas at 1 bar with a CO_2 concentration at about 10-16 percent in volume.[2] Current carbon capture technology is based on using chemical absorption by amines which is an effective technology to remove CO_2 from flue gas, but amine degradation, the high energy requirement in the regeneration process and corrosion in the system motivates alternative approaches.[3] These limitations have prompted significant investigation of physisorption for CO_2 separation which requires a porous material with high CO_2 affinity and capacity.[4, 5]

Recently, metal organic frameworks (MOFs) have received much attention due to their large surface areas, controllable pore structures, and versatile chemical compositions.[6-8] This class of porous materials is synthesized using organic linker molecules and metal joints that self-assemble to form crystalline materials with well-defined porous structures, high surface areas, and desired chemical functionalities.[9-11] The highly tuneable properties of MOFs make them good candidates in separation process, catalysis and gas adsorption applications. Most of the recent studies have been concentrated on the hydrogen and methane storage[12-17] some MOF materials show extremely high CO_2 capacity and very desirable isotherm

shapes also drawn considerable attention in CO_2 capture.[18-24] However, even if some MOF materials have good CO_2 uptake, for post-combustion capture applications it is more important to understand CO_2 adsorption in the low pressure region than at high pressures.[21, 25-27]

Given the large number of possible MOF topologies, linkers, and metal nodes, there are an almost unlimited number of MOFs that could be synthesized.[14] As a result, there is a requirement of developing techniques to characterize materials rapidly; using small sample quantities and that allow interpretation of the results easily, especially at low CO_2 partial pressure. Adsorption equilibrium measurements have traditionally been carried out by gravimetric or volumetric methods.[28] These techniques are straightforward and accurate, but they are time-consuming and require large amounts of adsorbents and are therefore not well-suited to adsorbent rapid screening studies, where absolute accuracy is less critical.

The original zero length column (ZLC) technique was introduced by Eic and Ruthven to study of adsorption kinetics.[29] The technique was then extended by Brandani et al. to the measurement of full adsorption isotherms.[30] The purpose of the present research was to develop a novel ZLC system designed for the study of novel adsorbents for carbon capture applications. A complete system should allow the ability to determine the adsorption capacity of novel materials, the mass transfer kinetics and the stability of the materials to impurities present in the flue gas. In this contribution we show how

a properly designed system can be used to measure CO_2 adsorption equilibrium on small samples.

EXPERIMENTAL

Adsorbent Materials

Most MOF materials are synthesized through solvothermal reactions. The synthesis procedures for the seven MOF samples used in our research are modified from the literature.[14, 31-33]

Mg/DOBDC (DOBDC = dioxybenzenedicarboxylate) was synthesized by the Matzger group at the University of Michigan. Linker precursor 2, 5-dihydroxyterephthalic acid (2.98 g) was dissolved in 180 mL 1-methyl-2-pyrrolidinone (NMP) + 20 mL deionized water using sonication. Mg (OAc) 2. $4H_2O$ (6.44 g) was added to a 0.5 L jar. The 2, 5-dihydroxyterephthalic acid solution was filtered into the jar. The solution was sonicated to dissolve completely the magnesium acetate and the jar was placed in a 120 °C oven for 20 hours. The mother liquor was decanted while still hot and the yellow solid was washed with methanol (3 × 200 mL). The methanol was decanted and replaced with fresh methanol (200 mL) three times over the course of three days. The yellow solid was evacuated at 250 °C for 16 hours and then transferred to a glove box for storage. One batch produced ~3 g of Mg/DOBDC.

Ni/DOBDC, nickel(II) acetate (18.7 g, 94.0 mmol, Aldrich) and 2,5-dihydroxyterephthalic acid (DOBDC, 37.3 g, 150 mmol, Aldrich) were placed in 1 L of mixed solvent consisting of equal parts tetrahydrofuran (THF) and deionized water. The mixture was then put into a 2 L static Parr reactor and heated at 110 °C for three days. The as-synthesized sample was filtered and washed with water. Then the sample was dried in air, and the solvent remaining inside the sample was exchanged with ethanol six times over eight days. Finally, the sample was activated at 150°C under vacuum with nitrogen flow.

Co/DOBDC, the reaction of cobalt (II) acetate and 2, 5-dihydroxyterephthalic acid ($C_8H_6O_6$) in a mixture of water and tetrahydrofuran (molar ratio 2:1:556:165) under autogenous pressure at 110°C in a Teflon-lined autoclave (50 percent filling level). This yielded a pink-red, needle-shaped crystalline substance $[Co_2(C_8H_2O_6)(H_2O)_2]8H_2O$. After the hypothetical removal of the noncoordinating solvent molecules in the channels, the empty channels occupy 49 percent of the total volume of the unit cell, and the average cross-sectional channel dimensions are 11.08×11.08 $Å^2$. The empty volume increases to 60 percent if the coordinating water is also removed. The water molecules excluding and including the coordinating water account for 29.2% and 36.6% of the mass, respectively.

HKUST-1(Cu-BTC) was produced by an electrochemical procedure, which is a new synthetic method compared to the previously reported synthesis under hydrothermal

conditions. The crystals obtained have double sided pyramidal shape and a size of maximum 6 μm.

The ZIF-8 pellets and Z1200 powder were made by and purchased from BASF.

The 5A and Silicalite power and 13X pellets are commercial materials. 13X-APG adsorbent is the sodium form of X zeolite possessing an aluminosilicate binder. 13X-APG adsorbent will adsorb molecules with critical diameters up to 8 angstroms. BET surface areas for the materials are reported in the supporting information.

Novel ZLC system

Figure 1shows a schematic diagram of the new semi-automated ZLC/breakthrough apparatus used in our experiments to measure the CO_2 capacity of novel adsorbents. Given the use of small samples of hydrophilic adsorbents it is very important to ensure that dry gases are used and individual drying columns, packed with silica gel and 5A zeolite, are present in each gas line. The gas-dosing volume consists of four stainless steel cylinders (1L each) inside an oven (Sanyo, Japan), which allows to prepare mixtures containing vapours.

In the flow control part, two sets of Brooks 5850S mass flow controllers were installed on the system. Both high flowrates (0-50 cc/min) and low flowrates (0-3 cc/min) are selected to allow kinetic and equilibrium measurements respectively. The

use of small samples and small gas flowrates reduces gas consumption in the experiment compared to other flow experiments, such as gravimetric systems or breakthrough apparatuses.

To ensure a smooth transition when switching the valves, a differential pressure transducer was installed to measure the pressure difference in the lines. The equilibration of the pressure in the lines is important for equilibrium measurements, since these are based on an accurate mass balance that assumes constant pressure in the system. The gases are passed through a preheat oven that is placed before the switch valves. The traditional rotary switch valve is replaced by four on-off valves installed between the preheat and the ZLC ovens eliminating the intermittent flow during the valve rotation and providing a smooth transition when switching gas flow to the column. The system can be easily modified to mount a larger column (up to grams of adsorbent) and run breakthrough experiments, but different mass flow controllers would be needed. Two needle valves are connected after the ZLC and on the vent line respectively to balance the pressure in order to avoid uneven flows when the valves are switched. The concentration at the outlet of the ZLC is measured using two detectors: an Ametek Dycor Dymaxion Residual Gas Analyzer mass spectrometer (MS) which samples less than 0.5 cc/min of gas and a GOW-MAC 24-527 thermal conductivity detector (TCD) with a Series 40 power supply and bridge control. The TCD requires a flow between 30 and 40 cc/min and when the ZLC is run at low flowrates a make-up flow of helium is used. The resulting gas stream going to the

TCD is then highly diluted and the electronics of the detector were modified in-house by adding a solid state amplifier and 50 Hz mains frequency filter to boost the signal to allow the analysis of the dynamic response.

A data acquisition and control system (National Instruments, USA) was used to acquire real-time data from the TCD and control the flowrates and oven temperatures. A user interface was developed in LabView to run the ZLC experiments in a semi-automated mode. The Ametek mass spectrometer is supplied with its own data acquisition software and allows studying multicomponent systems also.

Figure 2 shows the comparison of the blank experiments, i.e. the system without adsorbent, measured using the TCD. To achieve the same short-time response on the MS a capillary with a larger diameter of 0.06mm OD was used. The Ametek MS requires less than 0.5 cm^3/min of sample, which can be used in the low flowrate experiments without the need to add a make-up gas flow, so the signal is not diluted. Figure 2 also shows that the new ZLC system achieves a blank response with 90 percent approach to final equilibrium in approximately two seconds at a flowrate of 30 cm^3/min, which corresponds to a total volume of less than 0.44 cc without any solid in the column.

Special care needs to be taken at the lower flows to avoid the possibility of back flow or diffusion of air into the ZLC system, which would also bring water into the system. To avoid this, a short section of 1/16 in. tubing was added at the outlet and masses 32 and 28 were monitored with the MS to check for air leaks over the range of flowrates

used in the experiments. The narrow tubing is sufficiently short in order maintain a negligible pressure drop and the velocity in this section is sufficiently high to overcome the diffusion flux.

The ZLC cell is made of a Swagelok 1/8 in. fitting and the 10-15mg of sample is weighted in a Mettler-Toledo XS205 dual-range balance. While a traditional ZLC column is packed with 1-2 mg at one end of the union fitting, in this case a porous sinter disc is inserted at one end and the sample is loaded in the 9 mm internal section of the fitting and is sealed with a second porous sinter discs at the other end. The larger sample mass of 10-15 mg is used for the equilibrium capacity measurements.

The small amount of adsorbent required in the measurements is an important feature for rapid ranking of novel materials since only 20-30 mg need to be prepared for each batch. Prior to the experiment, the sample was regenerated by heating the sample with a ramping rate of 1°C/min to the required temperature and then held at this temperature for 12h with 1 cc/min of helium purge gas. After regeneration, the oven temperature is reduced to the desired temperature (i.e. 38°C for the standard CO_2 capacity tests) automatically. During an experiment, the sample was first equilibrated with a helium stream containing 10 percent by volume of CO_2. At time zero, the flow was switched to a pure helium purge stream at the same volumetric flow rate. For each sample, ZLC runs at two different flow rates were performed in the range of 1-3 cc/min to confirm the results. The low flowrate and increased sample size provide conditions for the ZLC desorption process to be controlled by equilibrium. For each flowrate replicate runs were performed and the fact that the curves at different

flowrates coincide on the Ft plot is an indication also that the samples do not loose capacity over time.

A LabView interface was programmed to carry out replicate experiments at different flowrates and the resulting semi-automated ZLC experiment is completed in less than one hour for all materials tested in this work.

THEORY

In a ZLC experiment, the column is short enough to be treated as a well-mixed cell with negligible external mass and heat transfer resistance. In a desorption experiment the differential mass balance is therefore given by:

$$V_s\frac{d\bar{q}}{dt}+V_g\frac{dc}{dt}+Fc=0 \qquad (1)$$

where V_g is the volume of gas; V_s represents the volume of solid; F is the volumetric flowrate; $\bar{q}$ is the average adsorbed phase concentration and c is the sorbate concentration in the gas phase. During the experiment the gas phase concentration is measured and the carrier flowrate is assumed constant.

Assuming linear equilibrium at the surface of the particles and mass transfer controlled by diffusion in a spherical geometry, the analytical solution is given by: [34]

$$\frac{c}{c_0}=2L\sum_{n=1}^{\infty}\frac{exp(-\beta_n{}^2 Dt/R^2)}{[\beta_n{}^2+\left(L-1-\gamma\beta_n{}^2\right)^2+L-1+\gamma\beta_n{}^2]} \qquad (2)$$

Where β_n are the positive roots of:

$$\beta_n\cot\beta_n+L-1-\gamma\beta_n^2=0 \qquad (3)$$

and

$$\gamma = \frac{V_g}{3KV_s} \tag{4}$$

$$L = \frac{1}{3}\frac{F}{KV_s}\frac{R^2}{D} \tag{5}$$

The parameter γ can be characterized as the ratio between the hold-up in the fluid phase and the accumulation in the solid. For gaseous systems it is generally very small and for γ < 0.1 the effect of the extra particle hold-up is negligible.[34]

The parameter L represents the ratio between the diffusional time constant and the "washout" of the solid phase. This parameter is essential in understanding how to design a ZLC system. At high purge flow rates or low sample mass (large values of L) the desorption rate is controlled by the diffusion of the sorbate out of the particle. At low purge flow rate or large sample mass, the residence time is large compared with the diffusional time constant (R^2/D) and the system is under equilibrium conditions.[35] When the parameter L is small the system becomes controlled by adsorption equilibrium and the response curve does not contain kinetic information. The use of the ZLC technique to rank materials based on equilibrium capacity measurements, therefore leads to the requirement that the experiments have to be carried out at low flow rates and relatively high sample mass to achieve equilibrium control.

For a linear isotherm one can assume

$$\bar{q} = q^* = Kc \tag{6}$$

and the desorption curve reduces to a simple exponential decay:[35]

$$\frac{c}{c_0} = \exp\left(\frac{-Ft}{KV_S + V_g}\right) \tag{7}$$

Eq. 7 shows that under equilibrium control all desorption curves at different flowrates will collapse into a single curve in a concentration vs Ft plot. This property is valid also when the isotherm is nonlinear and provides a very simple experimental check for equilibrium control.[36]

With the assumption that equilibrium is maintained between the gas and the solid phase; ideal gas behaviour; isothermal system; and a constant carrier flowrate, ie calculating the total flowrate as $F = F_c/(1-y)$, Eq. (1) is integrated to obtain:[36]

$$q^* = \left(\int_0^\infty \frac{y}{1-y} d\left(\frac{F_c t}{V_S}\right) - \int_0^t \frac{y}{1-y} d\left(\frac{F_c t}{V_S}\right) - \frac{V_g}{V_S} \cdot y\right) C \tag{8}$$

Where F_c is the flowrate of the carrier gas, y is the mole fraction and C is the total concentration which can be calculated from the ideal gas law, $C = \frac{P}{RT}$. While the flowrate of the carrier gas is not strictly constant, Eq. 8 is normally valid up to mole fractions of the adsorbate of 0.4-0.5.[37] Integration of Eq. 8 allows to calculate either the total capacity or the full adsorption isotherm. For strongly adsorbed components the exponential tail can be approximated by an analytical function and used to determine the integral more accurately.[38] We note that if the total capacity is the only information required, then the total mass balance holds even in if the system is kinetically controlled. The last term in the parenthesis is due to the hold-up in the gas phase and can be estimated separately from a blank experiment using an inert solid. Clearly as the solid capacity increases the effect of this term becomes progressively negligible. With systems that have even moderate capacity, Eq. 8 indicates that by

plotting the experimental results vs $\frac{Ft}{V_S}$, or the equivalent $\frac{Ft}{M}$ where M is the mass of the solid, will provide a very simple way to compare different materials as the area under the curve is nearly proportional to the adsorption capacity at the point of interest. This normalised plot allows to compare results from columns packed with different sample masses. Therefore even without detailed analysis of the results, a simple plot of the ZLC response curves allows to determine which materials have the larger CO_2 capacities.

RESULTS AND DISCUSSION

Figure 3 shows representative ZLC curves for 5A powder, 13X pellet, Ni/DOBDC powder and Mg/DOBDC powder at two different flowrates in both c vs t and c vs Ft plots. The overlap of curves in the Ft plot shows that the system is under equilibrium control. All the systems considered in this paper showed the same limiting behaviour at low flowrates and the curves shown are all under equilibrium control conditions, therefore the L parameter is always less than 1.

Figure 4 presents the ZLC ranking of CO_2 desorption curves at 0.1 bar and 38°C for all the MOFs and for three typical commercial zeolites. The areas under the desorption curves are a direct indication of the CO_2 adsorption capacity, as discussed in the theory section. It is clear from the plot that the ranking of the adsorbents is achieved by starting from right to left. The materials on the right side of the plot have

the highest capacities. The ZIF-8 pellets show a very low adsorption capacity for CO_2 at low partial pressures and in fact the desorption curve is effectively the same as that of a blank experiment and the curves were used to determine the volume of the gas phase, V_g = 0.36 cc, which is consistent with the result obtained for the empty column. As such, ZIF-8 is not a good candidate for post combustion carbon dioxide capture, but the curve is retained in the figure in order to show clearly that the capacity measured with less than 15 mg of sample for most materials is well above the limit of the measurement. By simply looking at the graph, which is a normalisation of the raw experimental data, it is possible to rank the materials as follows: Mg/DOBDC > Ni/DOBDC > 13X > 5A> Co/DOBDC> Cu/BTC > Silicalite > Z1200 > IRMOF-1 > ZIF-8. The simplicity of this analysis and result is a key advantage of the ZLC technique.

In addition to the simple ranking process based on the area under the curve in Figure 4, having confirmed that for all the systems considered the experiments were equilibrium controlled, it also possible to understand better the differences between the zeolites and the most promising MOFs. From the Ft plot in Figure 3 it is clear that the response of Ni/DOBDC and Mg/DOBDC is close to linear in the semi-logarithmic plot, ie in accordance with eq. 7, which indicates a linear isotherm. The curves for 5A and 13X zeolites present a clear non-linearity. The curves also show that the zeolites have a relatively high capacity at lower partial pressures, i.e. a much slower final exponential decay in proportion with the rest of the desorption curve. A good

candidate adsorbent for carbon capture should not only have a high CO_2 capacity, but also allow for ease of regeneration and in a vacuum swing adsorption (VSA) process the isothermal working capacity is maximum for a linear isotherm.[39] Figure 4 shows that for example zeolite 13X has comparable adsorption capacity to Ni/DOBDC, but most of the capacity for 13X is at a low pressure range, which means that in a commercial VSA cycle, 13X would require more energy in the low pressure/vacuum regeneration step than Ni/DOBDC and a lower vacuum pressure, or that the cycle for 13X would have to be operated at a higher temperature sacrificing the working capacity.

Given that the ZLC system is a flow through apparatus in an oven, it is possible to change the operating conditions and study also the temperature dependence of the Henry law constants, thus determining the limiting isosteric enthalpy of adsorption of adsorption. As an example,

Figure 5 shows the results at three different temperatures (65 °C, 50 °C and 38 °C) and two flowrates (1cc/min and 2cc/min) for Ni/DOBDC powder. From the slopes shown in the Ft plots, $KV_s + V_g$ can be calculated using Eq.7, and V_g can be obtained from the blank curve. The resulting parameters are summarized in Table 1. The limiting isosteric enthalpy of adsorption is obtained from the temperature dependence of KV_s/T, and a value of 39 kJ/mol was determined. It is important to note that for one system to determine the results at the reference condition and carry out the additional

runs at two temperatures required only one day of experimentation, including sample pre-treatment.

Having determined that the Ni/DOBDC and Mg/DOBDC MOFs were the most promising adsorbents, the powders were treated with steam as a preliminary stability check and also converted into pellets. The steaming treatment was performed using a small quantity of powder (< ½ cm height) which was loaded into quartz tubes and the material was heated to a specified temperature (150 °C) overnight in flow of nitrogen. The tubes were then allowed to cool to the designated steaming temperature (100 °C), and steam (in nitrogen) was introduced at the desired level (5%, 10% and 15%) for 2 hours. Pelletized Ni/DOBDC and Mg/DOBDC were pressed from pure powder samples without any binder using a manual press. An additional sample was prepared from the Ni/DOBDC powder using a small quantity of solvent to obtain a paste which was then extruded through a syringe. CO_2 capacities measured on these samples are compared in Figure 6 for Ni/DOBDC, 5 mole percent steaming has a mild negative effect on the CO_2 adsorption capacity. Based on the net analysis, it can be concluded that this steaming reduces capacity by approximately 16 percent, and pelletizing introduces an additional 11 percent capacity loss. But for up to 15 mole percent steaming, the reduction of the CO_2 adsorption capacity for Ni/DOBDC is up to 85 percent. Further, the results show that regeneration at room temperature and atmospheric pressure did not desorb all the water from Ni/DOBDC. For Mg/DOBDC, Figure 7 shows that the pelletization effect is only about a 7 percent capacity loss, but the steaming effectively deactivated the material. This set of

experiments show the application of the ZLC system to determine the relative effect of pelletization and steaming in direct comparison with the original MOF powders.

Figure 8 shows the final quantitative ranking of adsorbents from the numerical integration of the ZLC curves according to Eq. 8. The ranking order is in excellent agreement with that obtained from a gravimetric system[27] providing validation to the methodology used here, which requires significantly less experimental time, sample mass, gas consumption. The M/DOBDC and Cu/BTC MOFs contain unsaturated metal sites, which can interact with adsorbate molecules to increase CO_2 adsorption capacity, but the M/DOBDC (where M = Mg, Ni, or Co) MOFs have higher CO_2 adsorption capacity than Cu/BTC. This can be explained by the higher density of open metal sites (either per unit of surface area or per unit of free volume of material).[27] Compared with the other two M/DOBDC adsorbents, Mg/DOBDC performs particularly well. It is known that MgO exothermically chemisorbs CO_2 to form $MgCO_3$, but CO_2 is not chemisorbed by the Mg−O bonds in Mg/DOBDC because of the rigid nature of the framework that prevents insertion into the Mg−O bonds. However, the ionic character of this bond promotes a higher CO_2 uptake.[40] In M\DOBDC MOFs, the CO_2 adsorption capacity increases with decreasing M−O bond length in the framework. The order of these bond lengths, which may be considered as an indication of the affinity of metals in this coordination state toward oxygen, is Mg−O (1.969 Å) < Ni−O (2.003 Å) < Co−O (2.031 Å).[27]

CONCLUSIONS.

A novel semi-automated ZLC system has been developed to extend the technique to lower flowrates and slightly larger sample masses in order to optimise the experimental conditions for the rapid ranking of novel adsorbents in post-combustion carbon capture applications. There are several advantages over traditional gravimetric, volumetric and chromatographic systems, but the most important key aspect is that this system has been shown to arrive at reliable results with less than 15 mg of sample, which is essential when developing and testing novel materials.

At the point of interest for flue gas application (38 °C, 0.1 bar CO_2 partial pressure), the M/DOBDC class of MOFs was found to include excellent candidates for post-combustion carbon capture applications and in terms of capacity and shape of isotherm some outperform the benchmark zeolites.

To be able to determine the actual process performance, in addition to equilibrium studies it is also important to measure mass transfer kinetics and establish the stability of the novel materials to water and impurities present in flue gases. Given that the ZLC technique is a flow-through apparatus it is possible to carry out these additional experiments in-situ and parts 2 and 3 of this series will demonstrate how the new apparatus can provide also this information.

ACKNOWLEDGEMENTS

This project was supported by the U.S. Department of Energy through the National Energy Technology Laboratory under Award No. DE-FC26-07NT43092. However,

any opinions, findings, conclusions, or recommendations expressed herein are those of the authors and do not necessarily reflect the views of the DOE.

SUPPORTING INFORMATION AVAILABLE

Data on the BET surface areas and sample masses of the materials used are provided in the supporting information. This information is available free of charge via the Internet at http://pubs.acs.org/.

NOMENCLATURE

c = fluid-phase sorbate concentration (mol/m^3)

c_0 = initial fluid-phase sorbate concentration (mol/m^3)

C = total molar concentration (mol/m^3)

D = intracrystalline diffusion coefficient (m^2/s)

F = volumetric flowrate (m^3/s)

F_c = volumetric flowrate of the carrier gas (m^3/s)

ΔH = **limiting isosteric enthalpy of adsorption**

K = dimensionless Henry's law constant

K_P = Henry's law constant

L = dimensionless parameter defined in eq. 5

M = mass of solid (kg)

q = adsorbed-phase concentration (mol/m^3)

$\overline{q}$ = average adsorbed phase concentration (mol/m^3)

R = sorbent particle radius (m)

t = time (s)

V_s = volume of the solid in the ZLC cell (m^3)

V_g = volume of the gas in the ZLC cell (m^3)

y = mole fraction in the gas phase

β_n = roots of eq 3

γ = dimensionless parameter defined in eq. 4

REFERENCES

(1) IEA. *Energy Technology Transitions for Industry: Strategies for the Next Industrial Revolution.*; International Energy Agency: Paris, 2009.
(2) Orr, J. F. M. CO_2 capture and storage: are we ready? *Energ. Environ. Sci.* **2009**, 2, 449–458.
(3) Aaron, D.; Tsouris, C. Separation of CO_2 from Flue Gas: A Review. *Sep. Sci. Technol.* **2005**, 40, 321–348.
(4) Himeno, S.; Komatsu, T.; Fujita, S. High-Pressure Adsorption Equilibria of Methane and Carbon Dioxide on Several Activated Carbons. *J. Chem. Eng. Data* **2005**, 50, 369–376.
(5) He, Y. F.; Seaton, N. A. Heats of Adsorption and Adsorption Heterogeneity for Methane, Ethane, and Carbon Dioxide in MCM-41. *Langmuir* **2005**, 22,1150–1155.
(6) Wilmer, C. E.; Leaf, M.; Lee, C. Y.; Farha, O. K.; Hauser, B. G.; Hupp, J. T.; Snurr, R. Q. Large-scale screening of hypothetical metal–organic frameworks. *Nat. Chem.* **2012**, 4, 83–89.
(7) Furukawa, H.; Ko, N.; Go, Y. B.; Aratani, N.; Choi, S. B.; Choi, E.; Yazaydin, A. Ö.; Snurr, R. Q.; O'Keeffe, M.; Kim, J.; Yaghi, O. M. Ultrahigh Porosity in Metal-Organic Frameworks. *Science* **2010**, 329, 424–428.
(8) Li, H.; Eddaoudi, M.; O'Keeffe, M.; Yaghi, O. M. Design and synthesis of an exceptionally stable and highly porous metal-organic framework. *Nature* **1999**, 402, 276–279.
(9) Ferey, G. Hybrid porous solids: past, present, future. *Chem. Soc. Rev.* **2008**, 37, 191–214.
(10) Zaworotko, M. J. Materials science: Designer pores made easy. *Nature* **2008**, 451, 410–411.
(11) Ockwig, N. W.; Delgado-Friedrichs, O.; O'Keeffe, M.; Yaghi, O. M. Reticular Chemistry: Occurrence and Taxonomy of Nets and Grammar for the Design of Frameworks. *Accounts. Chem. Res.* **2005**, 38, 176–182.
(12) Ma, S.; Sun, D.; Simmons, J. M.; Collier, C. D.; Yuan, D.; Zhou, H.-C. Metal-Organic Framework from an Anthracene Derivative Containing Nanoscopic Cages Exhibiting High Methane Uptake. *J. Am. Chem. Soc.* **2007**, 130, 1012–1016.
(13) Rowsell, J. L. C.; Millward, A. R.; Park, K. S.; Yaghi, O. M. Hydrogen Sorption in Functionalized Metal Organic Frameworks. *J. Am. Chem. Soc.* **2004**, 126, 5666–5667.
(14) Rowsell, J. L. C.; Yaghi, O. M. Effects of Functionalization, Catenation, and Variation of the Metal Oxide and Organic Linking Units on the Low-Pressure Hydrogen Adsorption Properties of Metal Organic Frameworks. *J. Am. Chem. Soc.* **2006**, 128, 1304–1315.
(15) Fernandez, M.; Woo, T. K.; Wilmer, C. E.; Snurr, R. Q. Large-Scale Quantitative Structure-Property Relationship (QSPR) Analysis of Methane Storage in Metal-Organic Frameworks. *J. Phys. Chem. C* **2013**, 117, 7681–7689.
(16) Wilmer, C. E.; Farha, O. K.; Yildirim, T.; Eryazici, I.; Krungleviciute, V.; Sarjeant, A. A.; Snurr, R. Q.; Hupp, J. T. Gram-scale, high-yield synthesis of a robust

metal-organic framework for storing methane and other gases. *Energy Environ. Sci.* **2013**, 6, 1158–1163.
(17) Duan, X.; Yu, J. C.; Cai, J. F.; He, Y. B.; Wu, C. D.; Zhou, W.; Yildirim, T.; Zhang, Z. J.; Xiang, S. C.; O'Keeffe, M.; Chen, B. L.; Qian, G. D. A microporous metal-organic framework of a raresty topology for high CH_4 storage at room temperature. *Chem. Commun.* **2013**, 49, 2043–2045.
(18) Dybtsev, D. N.; Chun, H.; Yoon, S. H.; Kim, D.; Kim, K. Microporous Manganese Formate:A Simple Metal Organic Porous Material with High Framework Stability and Highly Selective Gas Sorption Properties. *J. Am. Chem. Soc.* **2003**, 126, 32–33.
(19) Natesakhawat, S.; Culp, J. T.; Matranga, C.; Bockrath, B. Adsorption Properties of Hydrogen and Carbon Dioxide in Prussian Blue Analogues $M_3[Co(CN)_6]_2$, M = Co, Zn. *J. Phys. Chem. C* **2006**, 111, 1055–1060.
(20) Li, J. R.; Yu, J. M.; Lu, W. G.; Sun, L. B.; Sculley, J.; Balbuena, P. B.; Zhou, H. C. Porous materials with pre-designed single-molecule traps for CO_2 selective adsorption. *Nat. Commun.* **2013**, 4, No. 1538.
(21) Xiang, S. C.; He, Y. B.; Zhang, Z. J.; Wu, H.; Zhou, W.; Krishna, R.; Chen, B. L. Microporous metal-organic framework with potential for carbon dioxide capture at ambient conditions. *Nat. Commun.* **2012**, 3, No. 954.
(22) Li, P. Z.; Wang, X. J.; Li, Y. X.; Zhang, Q.; Tan, R. H. D.; Lim, W. Q.; Ganguly, R.; Zhao, Y. L. Co(II)-tricarboxylate metal-organic frameworks constructed from solvent-directed assembly for CO_2 adsorption. *Micropor. Mesopor. Mat.* **2013**, 176, 194–198.
(23) Lau, C. H.; Babarao, R.; Hill, M. R. A route to drastic increase of CO_2 uptake in Zr metal organic framework UiO-66. *Chem. Commun.* **2013**, 49, 3634–3636.
(24) Remy, T.; Peter, S. A.; Van der Perre, S.; Valvekens, P.; De Vos, D. E.; Baron, G. V.; Denayer, J. F. M. Selective Dynamic CO_2 Separations on Mg-MOF-74 at Low Pressures: A Detailed Comparison with 13X. *J. Phys. Chem. C* **2013**, 117, 9301–9310.
(25) Millward, A. R.; Yaghi, O. M. Metal Organic Frameworks with Exceptionally High Capacity for Storage of Carbon Dioxide at Room Temperature. *J. Am. Chem. Soc.* **2005**, 127, 17998–17999.
(26) Park, J.; Kim, H.; Han, S. S.; Jung, Y. Tuning Metal-Organic Frameworks with Open-Metal Sites and Its Origin for Enhancing CO_2 Affinity by Metal Substitution. *J. Phys. Chem. Lett.* **2012**, 3, 826–829.
(27) Yazaydin, A. O.; Snurr, R. Q.; Park, T.-H.; Koh, K.; Liu, J.; LeVan, M. D.; Benin, A. I.; Jakubczak, P.; Lanuza, M.; Galloway, D. B.; Low, J. J.; Willis, R. R. Screening of Metal-Organic Frameworks for Carbon Dioxide Capture from Flue Gas Using a Combined Experimental and Modeling Approach. *J. Am. Chem. Soc.* **2009**, 131, 18198–18199.
(28) Han, S. G.; Huang, Y. G.; Watanabe, T.; Dai, Y.; Walton, K. S.; Nair, S.; Sholl, D. S.; Meredith, J. C. High-Throughput Screening of Metal-Organic Frameworks for CO_2 Separation. *ACS Comb. Sci.* **2012**, 14, 263–267.

(29) Eic, M.; Ruthven, D. M. A new experimental technique for measurement of intracrystalline diffusivity. *Zeolites* **1988**, 8, 40–45.
(30) Brandani, F.; Ruthven, D. M.; Coe, C. G. Measurement of Adsorption Equilibrium by the Zero Length Column (ZLC) Technique Part 1:Single-Component Systems. *Ind. Eng. Chem. Res.* **2003**, 42, 1451–1461.
(31) Rosi, N. L.; Kim, J.; Eddaoudi, M.; Chen, B.; O'Keeffe, M.; Yaghi, O. M. Rod Packings and Metal-Organic Frameworks Constructed from Rod-Shaped Secondary Building Units. *J. Am. Chem. Soc.* **2005**, 127, 1504–1518.
(32) Wong-Foy, A. G.; Matzger, A. J.; Yaghi, O. M. Exceptional H_2 Saturation Uptake in Microporous Metal Organic Frameworks. *J. Am. Chem. Soc.* **2006**, 128, 3494–3496.
(33) Dietzel, P. D. C.; Morita, Y.; Blom, R.; Fjellvåg, H. An In Situ High-Temperature Single-Crystal Investigation of a Dehydrated Metal–Organic Framework Compound and Field-Induced Magnetization of One-Dimensional Metal–Oxygen Chains. *Angew. Chem. Int. Ed.* **2005**, 44, 6354–6358.
(34) Brandani, S.; Ruthven, D. M. Analysis of ZLC desorption curves for liquid systems. *Chem. Eng. Sci.* **1995**, 50, 2055–2059.
(35) Brandani, S.; Ruthven, D. M. Analysis of ZLC desorption curves for gaseous systems. *Adsorption* **1996**, 2,133–143.
(36) Wang, H.; Brandani, S.; Lin, G.; Hu, X. Flowrate Correction for the Determination of Isotherms and Darken Thermodynamic Factors from Zero Length Column (ZLC) Experiments. *Adsorption* **2011**, 17, 687–694.
(37) Ruthven, D. M.; Farooq, S.; Knaebel, K. S., *Pressure Swing Adsorption*. VCH: New York, 1994.
(38) Brandani, S.; Ruthven, D. M. Moments Analysis of the Zero Length Column Method. *Ind. Eng. Chem. Res.* **1996**, 35, 315–319.
(39) Caskey, S. R.; Wong-Foy, A. G.; Matzger, A. J. Dramatic Tuning of Carbon Dioxide Uptake via Metal Substitution in a Coordination Polymer with Cylindrical Pores. *J. Am. Chem. Soc.* **2008**, 130, 10870–10871.
(40) Britt, D.; Furukawa, H.; Wang, B.; Glover, T. G.; Yaghi, O. M. Highly efficient separation of carbon dioxide by a metal-organic framework replete with open metal sites. *Proc. Natl. Acad. Sci. U. S. A.* **2009**, 106, 20637–20640.

Figures

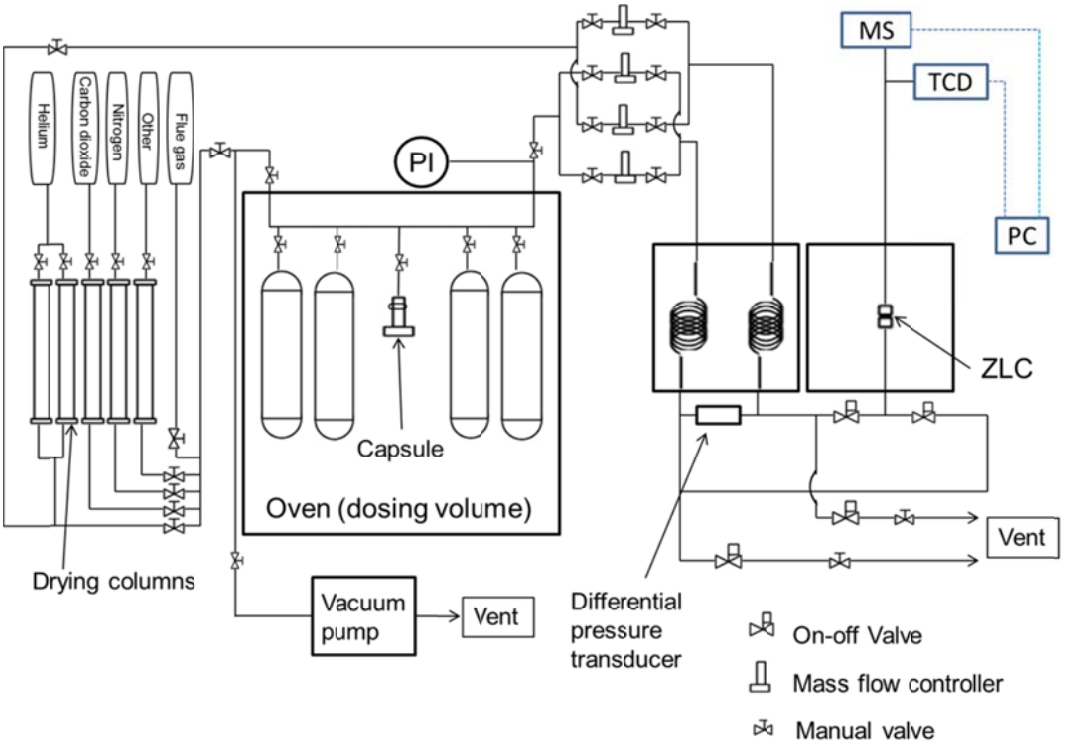

Figure 1. Schematic diagram of the experimental system showing details of the developed semi-automated zero length column system.

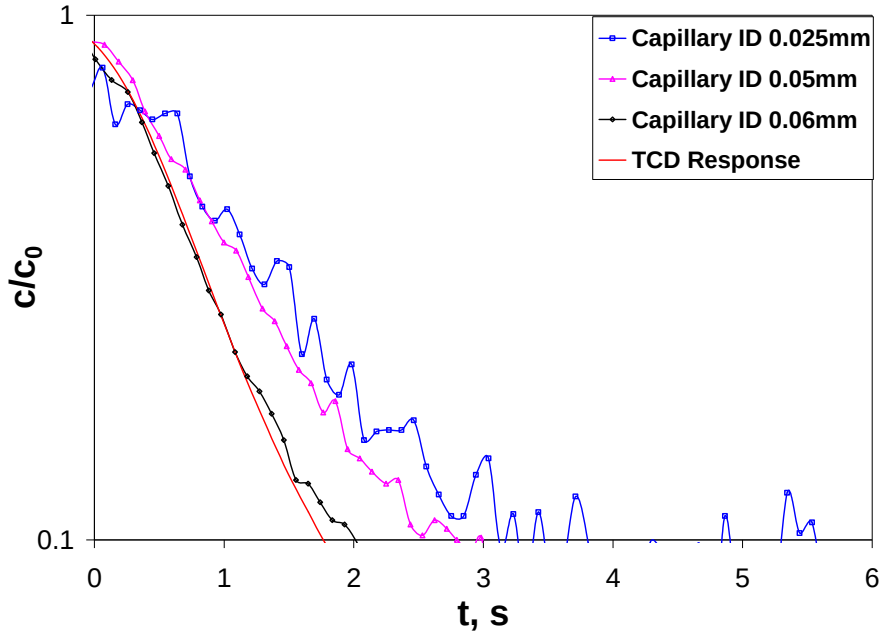

Figure 2. ZLC response of blank runs with the two detectors at the flowrate of 30 cc/min.

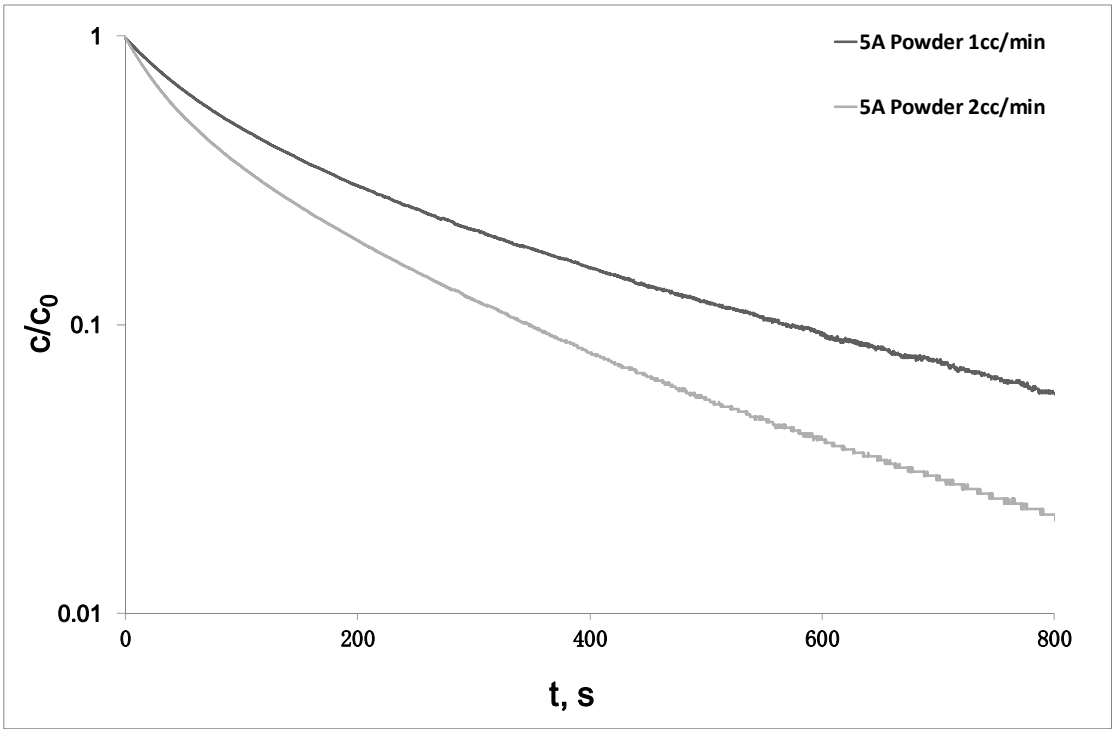
1
0.1
0.01
c/c0
0
200
400
600
800
t, s
5A Powder 1cc/min
5A Powder 2cc/min

(a)

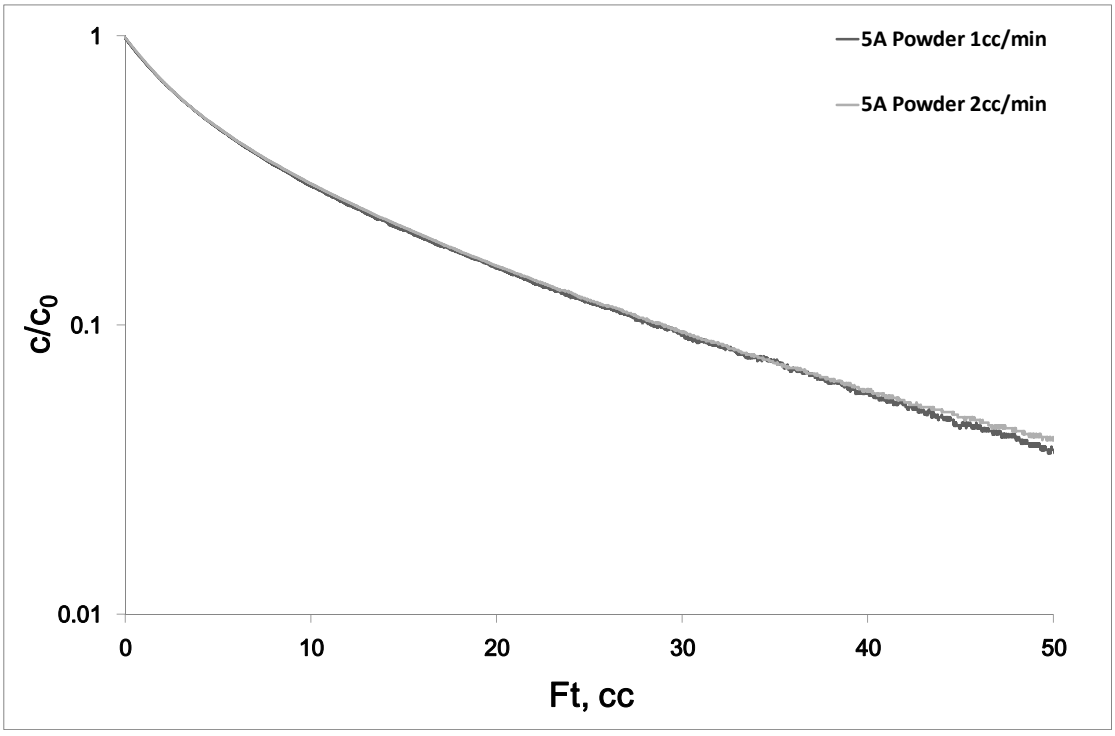
1
0.1
0.01
c/c0
0
10
20
30
40
50
Ft, cc
5A Powder 1cc/min
5A Powder 2cc/min

(b)

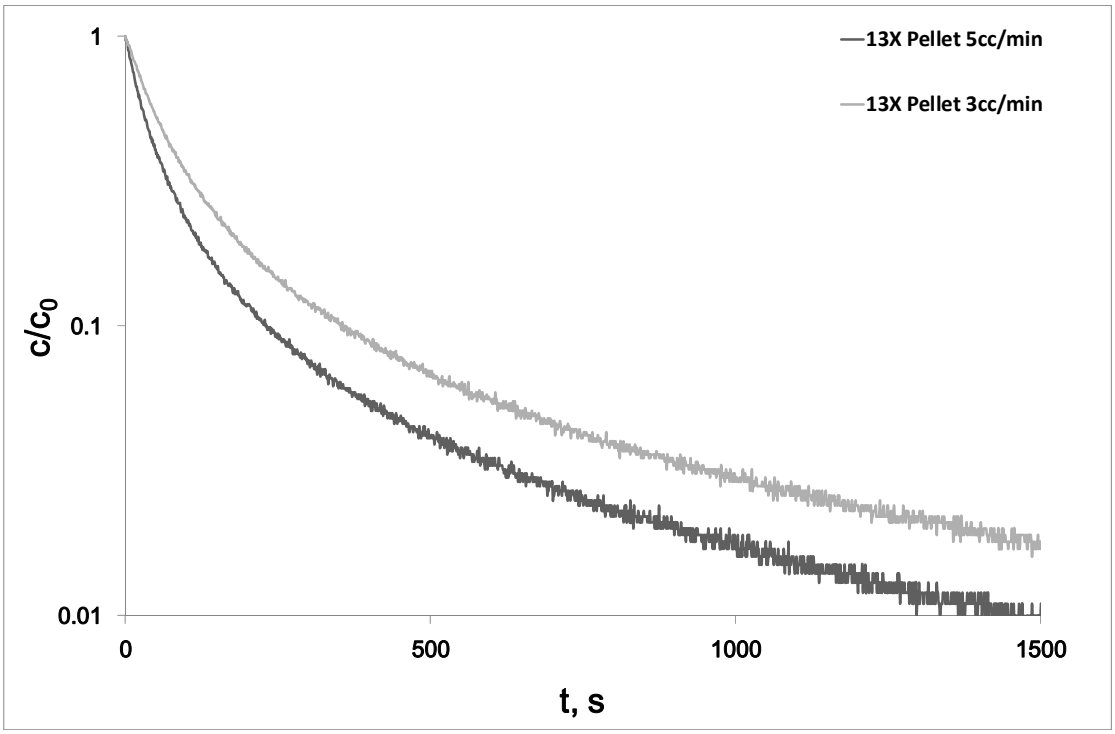
13X Pellet 5cc/min
13X Pellet 3cc/min
1
0.1
0.01
c/c0
0
500
1000
1500
t, s

(c)

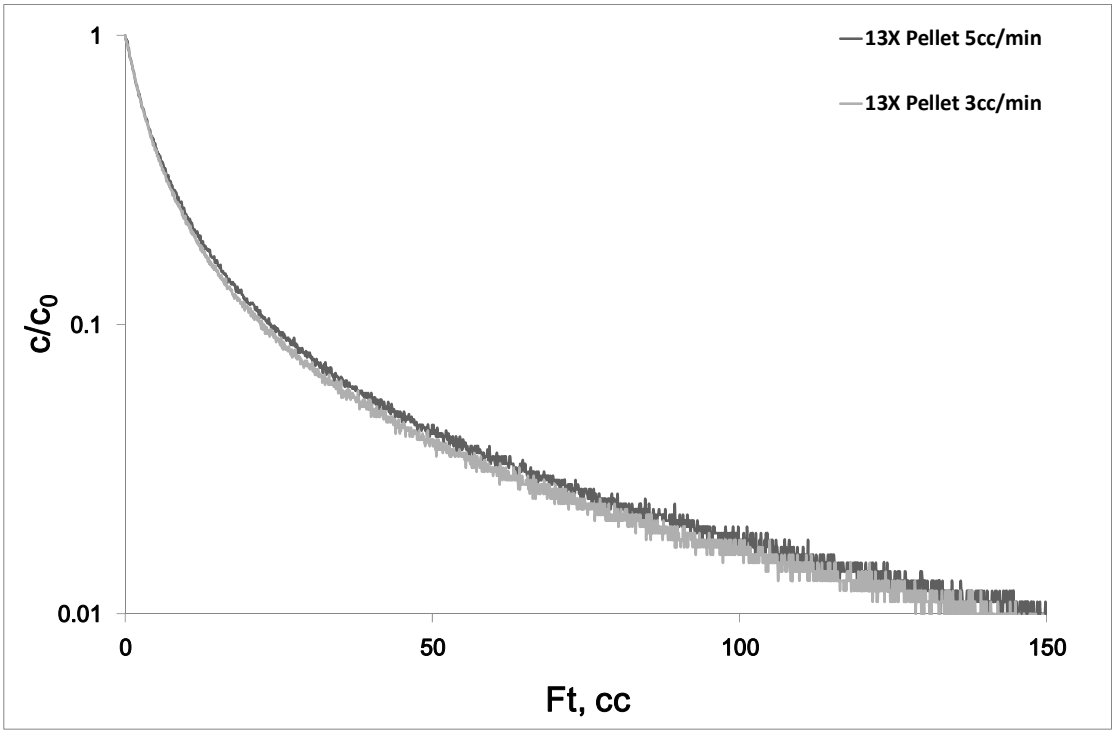
13X Pellet 5cc/min
13X Pellet 3cc/min
1
0.1
0.01
c/c0
0
50
100
150
Ft, cc

(d)

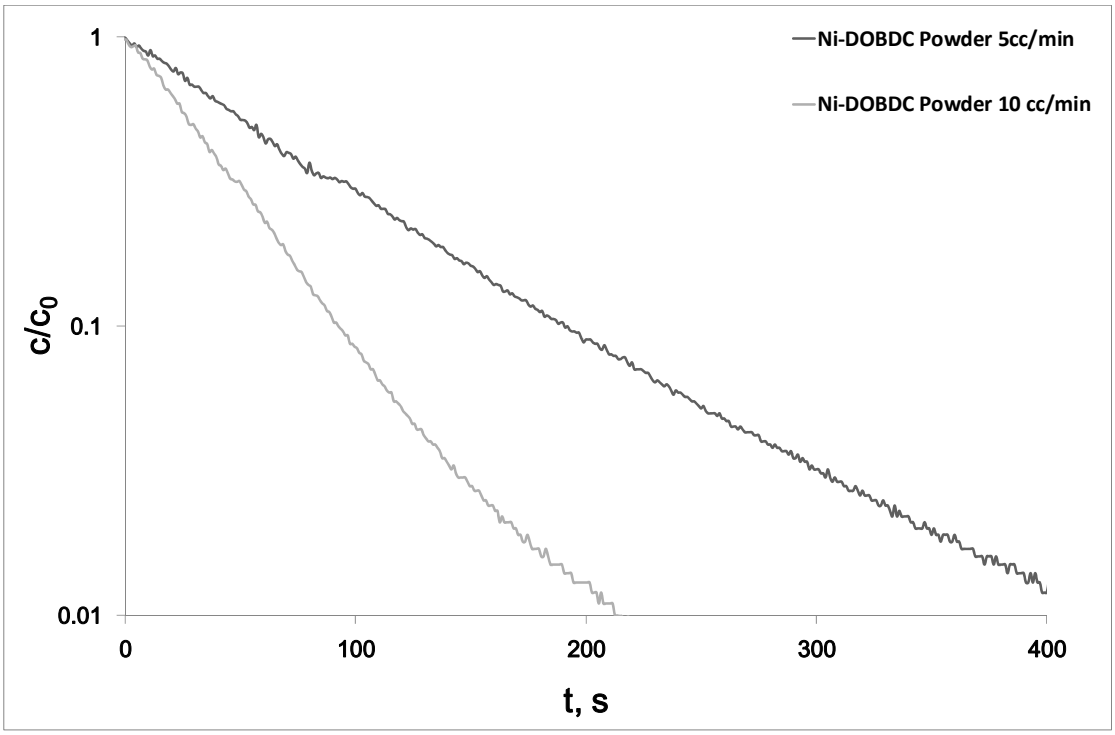
Ni-DOBDC Powder 5cc/min
Ni-DOBDC Powder 10 cc/min
1
0.1
0.01
c/c0
0
100
200
300
400
t, s

(e)

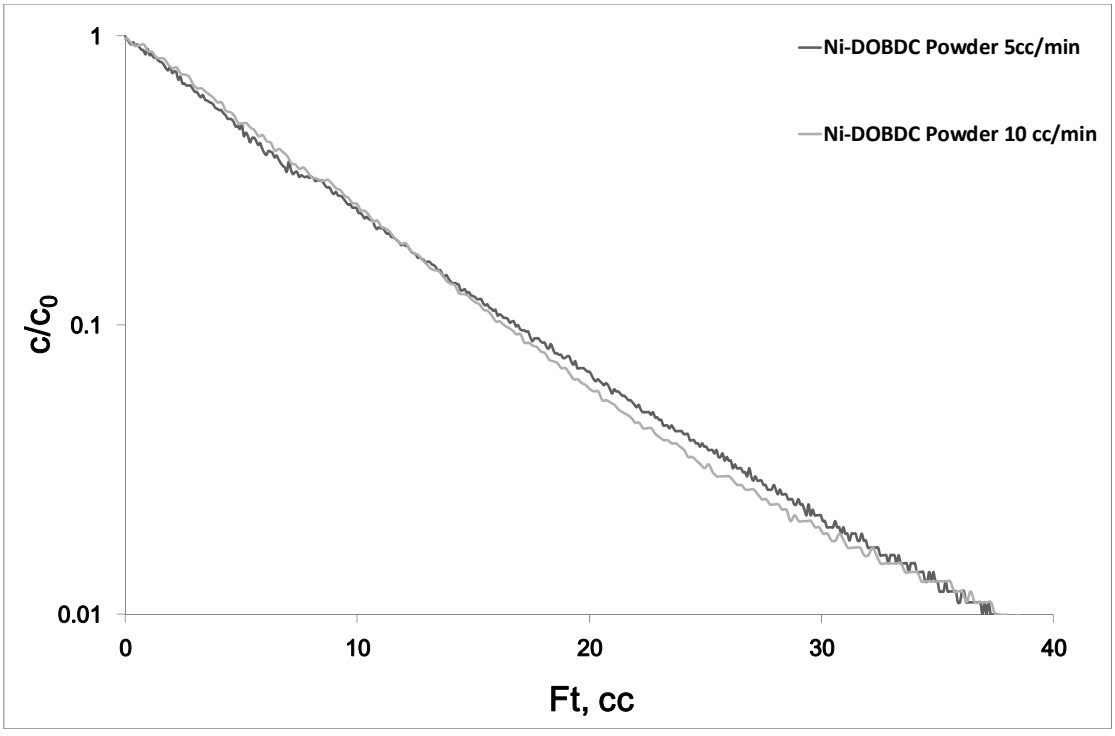
Ni-DOBDC Powder 5cc/min
Ni-DOBDC Powder 10 cc/min
1
0.1
0.01
c/c0
0
10
20
30
40
Ft, cc

(f)

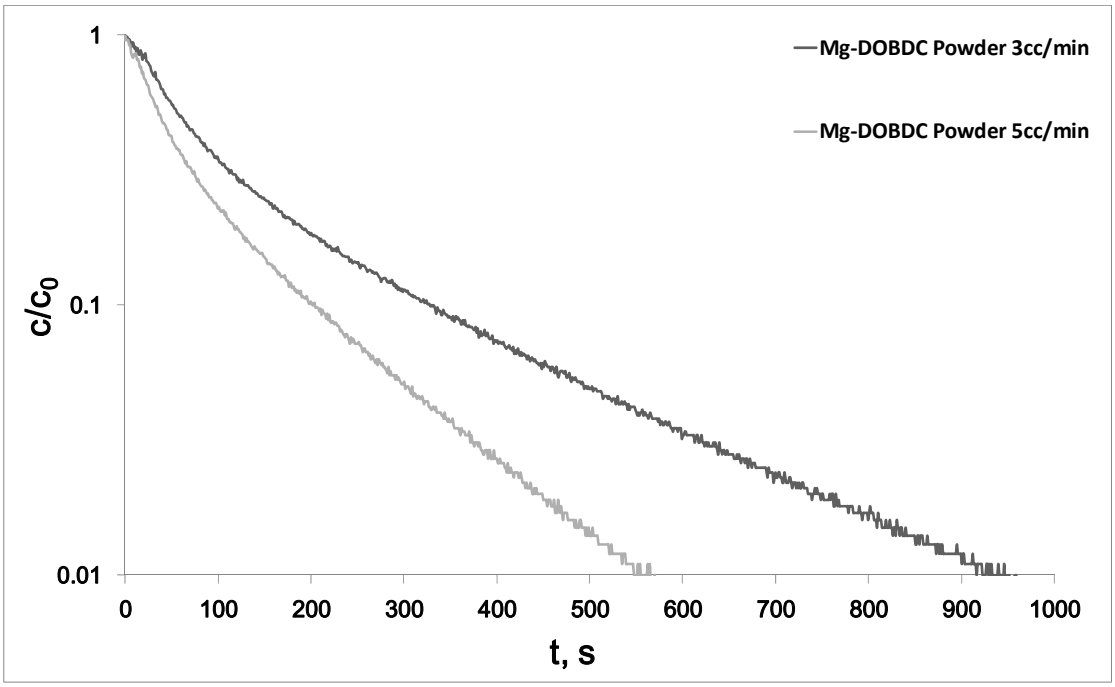

(g)

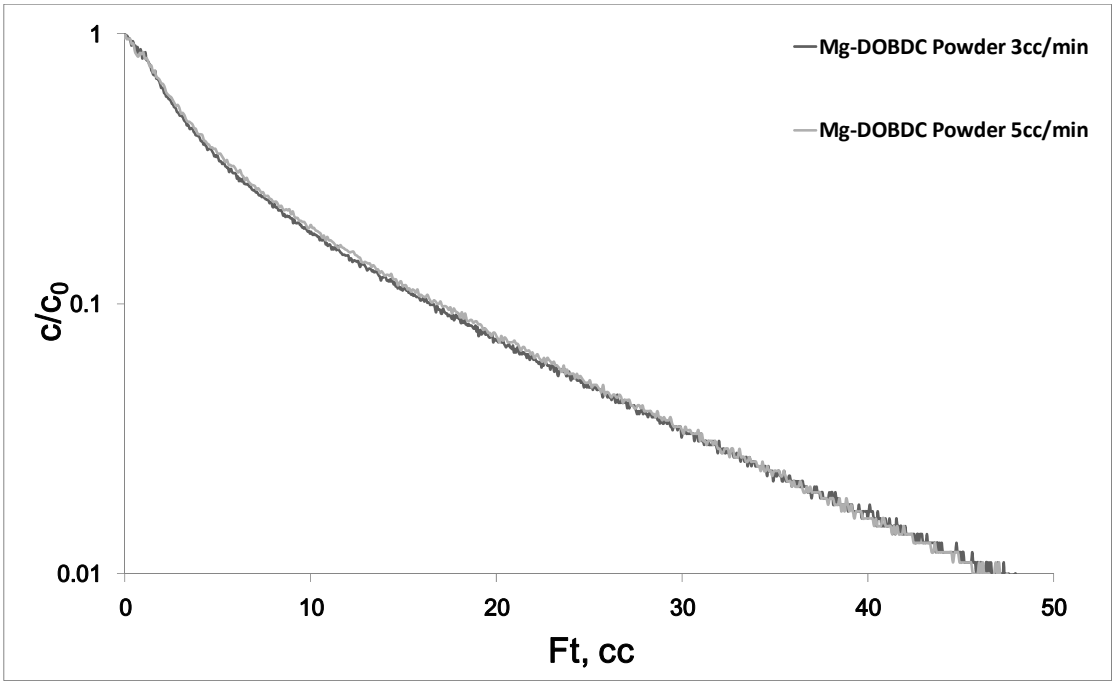

(h)

Figure 3. Experimental ZLC response curves and Ft curves of 5A powder (a,b), 13X pellet (c,d), Ni/DOBDC powder (e,f) and Mg/DOBDC powder (g,h) at two different flowrates and at 0.1bar of CO_2 in helium and 38 °C.

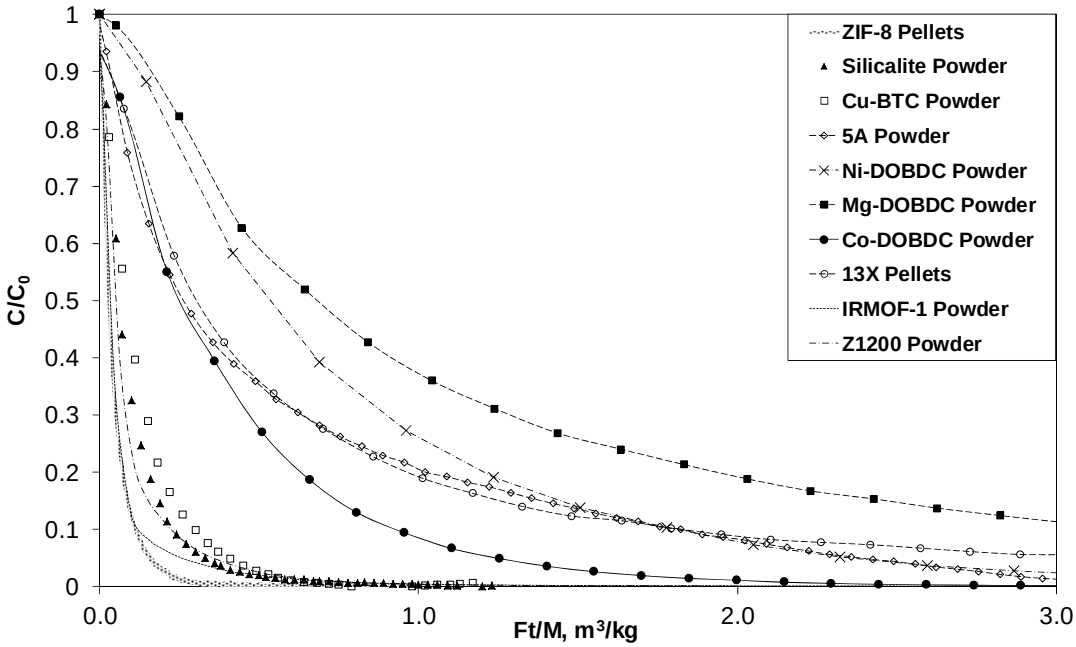

Figure 4. Ranking of all adsorbents at the point of interest for flue gas application (38 °C, 0.1 bar CO_2 partial pressure). Sample masses are reported in the Supporting Information.

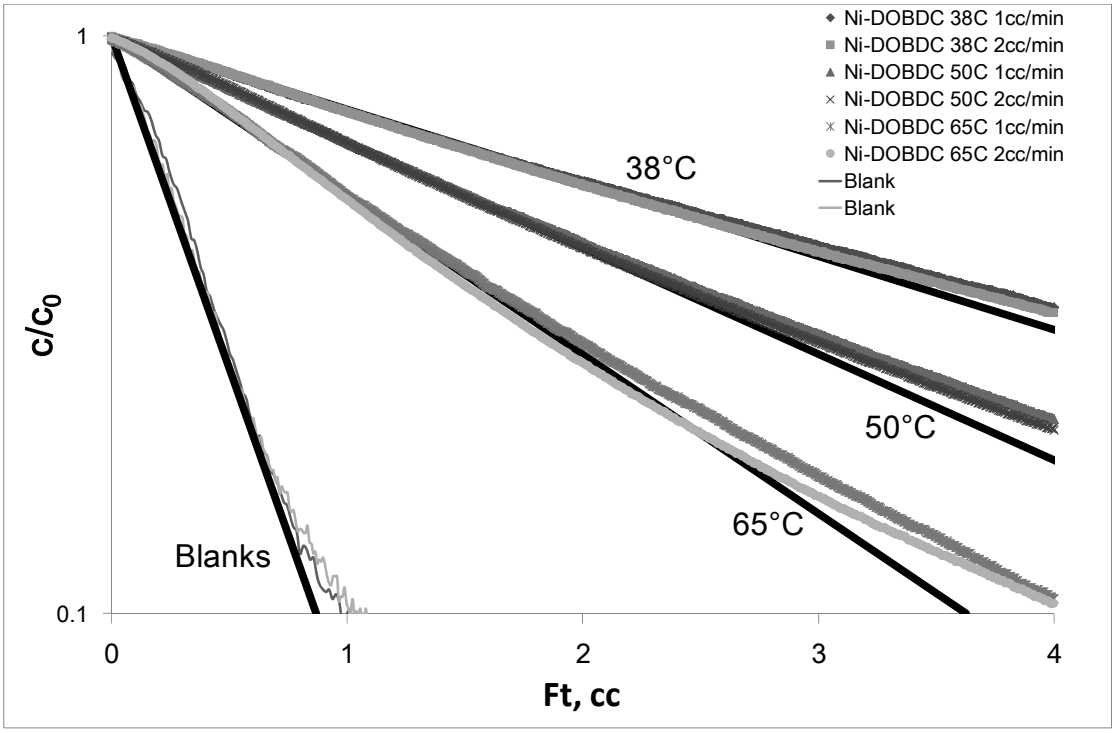

Figure 5. Experimental Ft plot with linear asymptotes (Henry's Law region) of Ni/DOBDC powder at 0.1bar of CO_2 in helium, 38 °C, 50 °C and 65 °C, 1 and 2 cc/min and blanks.

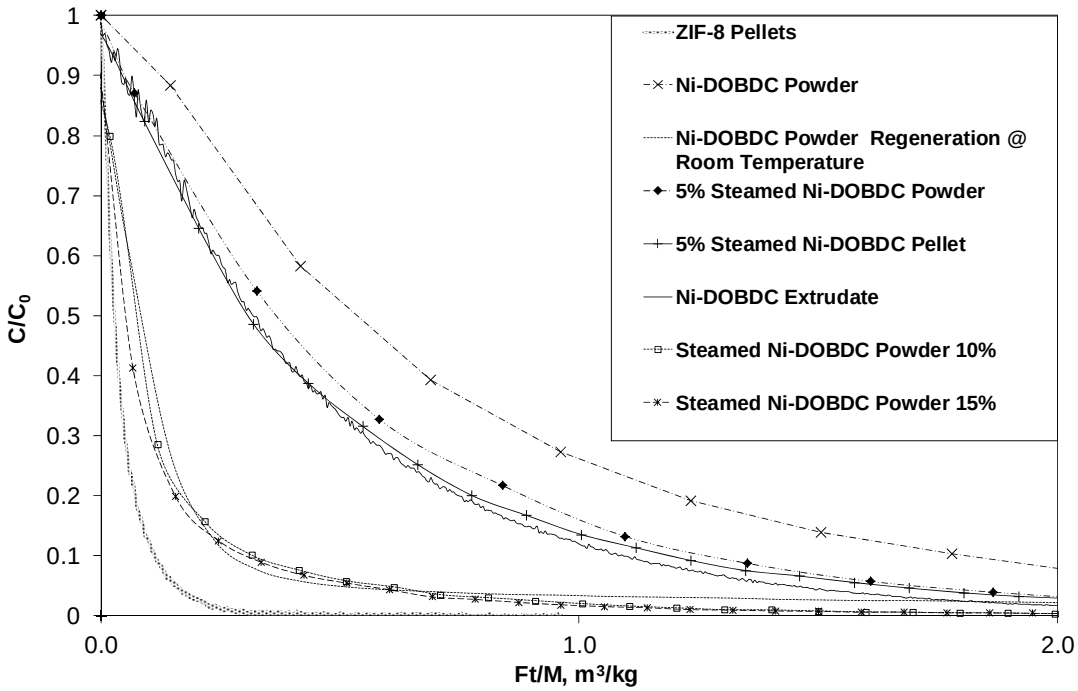

Figure 6. Comparison of Ni-DOBDC samples under different modifications (38 °C, 0.1 bar CO_2 partial pressure).

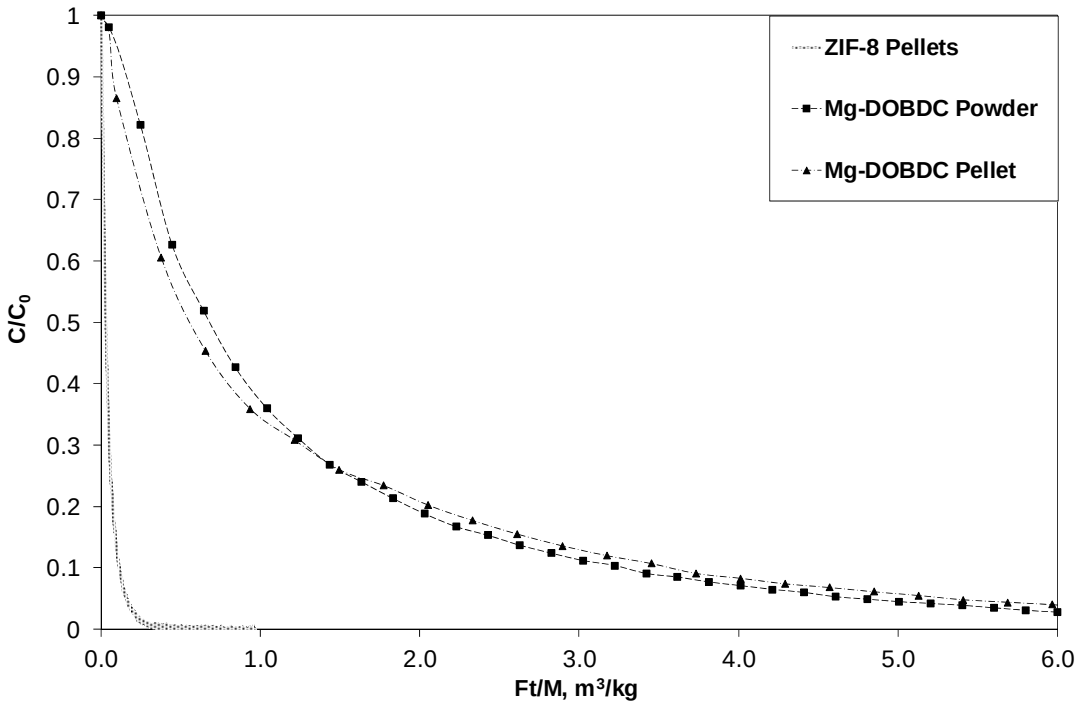

Figure 7. Comparison of Mg-DOBDC samples under different modifications (38 °C, 0.1 bar CO_2 partial pressure).

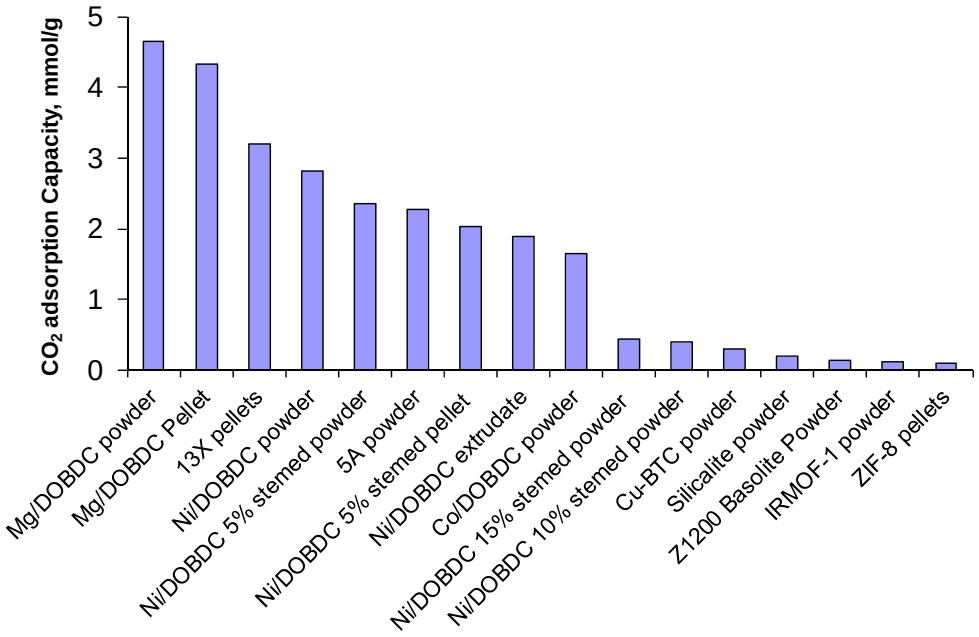

Figure 8. Experimental CO_2 capacity calculated from ZLC in screened adsorbent at 0.1 bar, data obtained at 38 °C.

Table 1. Summary of parameters obtained from the analysis of the curves shown in Fig. 5 to determine the limiting isosteric enthalpy of adsorption.

T (K)	V_g (cc) from blank	KV_s (cc) from eq. 7	ΔH (kJ/mol)
311.15	0.36	2.89	39
323.15		1.86	
338.15		0.95	

For Table of Contents Only